ChemPubSoc Europe

DOI: 10.1002/chem.201805051

CHEMISTRY
A European Journal
Full Paper

Nerve Agents

Reversal of Tabun Toxicity Enabled by a Triazole-Annulated Oxime Library—Reactivators of Acetylcholinesterase

Zrinka Kovarik[+],[b] Jarosław Kalisiak[+],[c] Nikolina Maček Hrvat,[b] Maja Katalinić,[b] Tamara Zorbaz,[b] Suzana Žunec,[b] Carol Green,[d] Zoran Radić,[a] Valery V. Fokin,[c, e] K. Barry Sharpless,[c] and Palmer Taylor*[a]

Abstract: Acetylcholinesterase (AChE), an enzyme that degrades the neurotransmitter acetylcholine, when covalently inhibited by organophosphorus compounds (OPs), such as nerve agents and pesticides, can be reactivated by oximes. However, tabun remains among the most dangerous nerve agents due to the low reactivation efficacy of standard pyridinium aldoxime antidotes. Therefore, finding an optimal reactivator for prophylaxis against tabun toxicity and for post-exposure treatment is a continued challenge. In this study, we analyzed the reactivation potency of 111 novel nucleophilic oximes mostly synthesized using the CuAAC triazole ligation between alkyne and azide building blocks. We identified several oximes with significantly improved in vitro reactivating potential for tabun-inhibited human AChE, and in vivo antidotal efficacies in tabun-exposed mice. Our findings offer a significantly improved platform for further development of antidotes and scavengers directed against tabun and related phosphoramidate exposures, such as the Novichok compounds.

Introduction

Toxicity and mortality associated with nerve agents arise primarily from irreversible inhibition of acetylcholinesterase (AChE; EC 3.1.1.7), an enzyme whose role is essential in cholinergic neurotransmission. Inhibition of AChE activity results in accumulation of the neurotransmitter acetylcholine at vital cholinergic sites, which in turn leads to life-threatening toxic manifestations. Currently used therapies rely on anticholinergic (atropine) agents and oximes as reactivators of inhibited AChE[1] along with anti-seizure agents. However, this approach has limitations, one of which is the inability of currently applied standard oximes (TMB-4, obidoxime, HI-6 and 2-PAM) to efficiently reactivate AChE inhibited by certain organophosphates.[2] Current therapy is particularly ineffective in case of tabun. Tabun is a highly toxic organophosphorus compound (OP) and nerve agent of warfare and terrorism originally developed as a pesticide in Germany in 1936. An electron pair located on the phosphoramido group of tabun prevents efficient nucleophilic attack by oximates (Figure 1).[3] In addition, the active center gorge of the tabun-AChE conjugate is sterically congested, thus reducing access of the oxime to the phosphorus center.[4] Accordingly, phosphoramide conjugates show resistance to the classical reactivators. Among standard oximes, TMB-4 shows the highest reactivation potency in test cases of tabun inhibition.[2d] However, it is also the most toxic among the four, prompting further search for efficient tabun reactiva-

[a] Dr. Z. Radić, Prof. P. Taylor
Skaggs School of Pharmacy and Pharmaceutical Sciences
University of California at San Diego
La Jolla, CA 92093-0650 (USA)
E-mail: pwtaylor@ucsd.edu

[b] Dr. Z. Kovarik,[+] Dr. N. M. Hrvat, Dr. M. Katalinić, T. Zorbaz, Dr. S. Žunec
Institute for Medical Research and Occupational Health
HR-10000 Zagreb (Croatia)

[c] Dr. J. Kalisiak,[+] Dr. V. V. Fokin, Prof. K. B. Sharpless
Skaggs Institute for Chemical Biology
The Scripps Research Institute
La Jolla, CA 92037 (USA)

[d] Dr. C. Green
SRI International
Menlo Park, CA 94025-3493 (USA)

[e] Dr. V. V. Fokin
The Bridge@USC
University of Southern California
Los Angeles, CA 90089 (USA)

[+] These authors contributed equally to this work.

Supporting information and the ORCID identification number(s) for the author(s) of this article can be found under: https://doi.org/10.1002/chem.201805051.

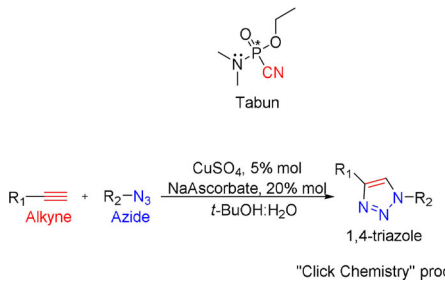

Figure 1. Structure of racemic nerve agent tabun, (R/S)-ethyl *N*,*N*-dimethylphosphoramido cyanidate, and general Scheme of CuAAC employed to synthesize oxime library tested for the antidotal activity against tabun.

tors.[1b,5] Our previous studies on pyridinium and imidazolium oximes show that only pyridinium oximes with *para*-positioned oxime group possess sufficient potency to reactivate tabun-inhibited AChE. Particularly effective were K074, K075 and K203, with overall reactivation rate constants about seven times higher than that of TMB-4 and about four times higher than with K048, their analogue sharing a similar butylene linker.[2d,4c,6]

Click chemistry enables rapid synthesis of molecular libraries from readily available building blocks[7] for in vitro and in vivo development of a landscape of agents to counteract OP exposure. Herein, we report design and synthesis of over 100 oximes, mainly those encompassing a triazole ring synthesized using the copper(I)-catalyzed azide-alkyne cycloaddition (CuAAC) to form a linking 1,4-triazole (Figure 1). The library was screened for oxime-dependent reactivation kinetics of tabun-, VX-, sarin-, cyclosarin-, and paraoxon- inhibited human recombinant AChE. Several novel oximes were particularly efficient reactivators in tabun inhibition. The lead compounds were investigated in vivo. Since these oximes present an incompletely studied structural scaffold, we also tested their cytotoxicity on neuroblastoma cell line, SH-SY5Y. Our findings offer a platform for further development of more efficacious antidotes not only for counteracting tabun, but also exposure to related nerve agents.

Results

Chemistry

Our search for efficient reactivators of phosphylated AChE was facilitated by rapid synthesis of a large number of candidate compounds using CuAAC reaction (Figure 1). For this study, in addition to 1,4-triazole-oximes (**1A–62A**) obtained by CuAAC, a series of *N*-alkyl-2 pyridinium compounds (**1B–5B**), some of which contain more complex *N*-alkyl substituents (**1C–17C**) and a series of miscellaneous oximes (**1D–27D**) were synthesized (chemical structure of all oximes are given in Table 3, Appendix). Owing to the nearly quantitative yields in all of the triazole linkage steps, libraries of candidate compounds were directly employed in the initial reactivation screens. Most structurally characterized compounds were then made in 10–30 mg quantities; those used for in vivo efficacy and pharmacokinetics experiments were synthesized in quantities from 100 mg to several grams. Some of triazole aldoxime compounds of little or no activity were screened directly as reaction mixtures as described previously.[7c] All of the compounds were prepared in good yields and were characterized by standard analytical spectroscopy methods (1D and 2D NMR, IR, MS, elemental analysis). Supporting Information details synthetic and characterization data.

Reactivation of human recombinant AChE inhibited by tabun

The novel oximes, partially presented in Cochran et al.,[7c] were tested as reactivators of human recombinant AChE inhibited by tabun (Figure 1), phosphoramide compounds with cyanide leaving group that show resistance to the classical reactivators. The oxime library was screened initially at a single oxime concentration for reactivation of tabun-conjugated AChE. Since some of the oximes exhibited a high binding affinity for AChE resulting in inhibition of its activity, their reactivation rates were assayed at lower concentrations. We employed a high percentage of reactivation achieved within a short time as the main criterion for selection among the oximes. Out of 111 novel oximes, 40 were deemed more efficient reactivators of AChE than 2-PAM and were then ranked in terms of the observed reactivation rate (k_{obs}), as shown in Figure 2 and Table 3 (Appendix). Although reactivation was monitored up to 24 h, restoration of enzyme activity approaching 100% was evident in only 9 of these oximes, while maximal reactivation of greater than 50% was found for 59 oximes. Six novel triazole compounds were more efficient in the screening than obidoxime.[8] Under our experimental conditions, which employed a 10-fold excess of OP over AChE for its inhibition, it is likely that one enantiomer of the racemic tabun reacted preferentially with AChE (Figure 1), because of steric differences between R_P and S_P conjugates fitting into the spatially constrained acyl pocket of AChE.[9a,b] We expected dominant (>90%) formation of a single tabun-AChE conjugate. Restoration of the full 100% of the AChE activity may have required reactivation of both diastereomeric conjugates of the serine-linked phosphoester, including the one of lower prevalence formed with the less reactive enantiomer. Although this explanation is plausible, inherent experimental variability in our assay precludes us from emphasizing this detail in order to avoid over-interpretation of our data.

As detailed in Table 3 (Appendix), maximal reactivation was equal or less than 20% for 41 of the oximes, and the observed reactivation rate constant was not calculated. Compounds with low reactivation rates and a lower percentage of reactivation, in our view, do not provide data for precise quantitation. In addition, we determined the degree of reversible inhibition by oximes for AChE by assessing enzyme activity when not exposed to tabun. Of the 111 oximes, 99 exhibited some inhibitory potency at 0.01 mM: 37 of which inhibited AChE less than 30%, 31 oximes inhibited AChE between 30 and 50%, 26 oximes between 50 and 80%, and 17 oximes more than 80% (Table 3, Appendix). The additional 12 oximes, identified as strong reversible inhibitors of AChE, inhibiting more than 95% at 0.01 mM concentration, were re-examined at 5–50-fold lower oxime concentrations, where they displayed inhibitory potencies between 10 and 85%.

For the most efficient oximes that reactivated AChE approaching completion within short time, we ran reactivation kinetics over a concentration range of the oximes enabling us to deconstruct reactivation constants. Reactivation constants involved in the two-step reactivation mechanism (equilibrium binding followed by the irreversible reactivation) are shown in Figure 3. In Table 1, results are arranged by the second-order rate constants since the reactivation efficiency depends not only on the rate of displacement of conjugated tabun regenerating the original activity, but also on the apparent affinity

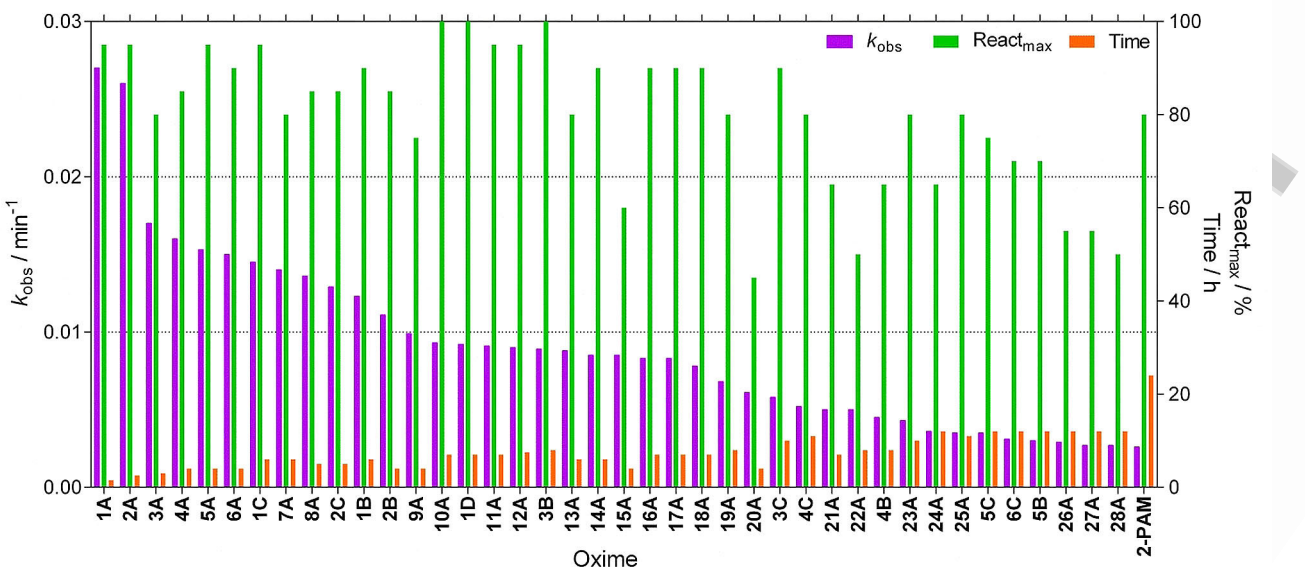

Figure 2. Reactivation screening of tabun-inhibited AChE by 40 out of 111 oximes with higher reactivation efficacy (k_{obs}) than 2-PAM. Oximes were 1 mM in the reactivation buffer, except 0.2 mM **3A** and 0.1 mM **9A**, **22A**, **23A** and **25A** due to reversible high affinity for binding. Presented values are means of at least three experiments (standard errors were less than 10%). The rate constants for reactivation, k_{obs}, are shown in purple, maximal estimated reactivation percentages in green, and the approximate times to achieve maximum plateau values at the given oxime concentration in orange.

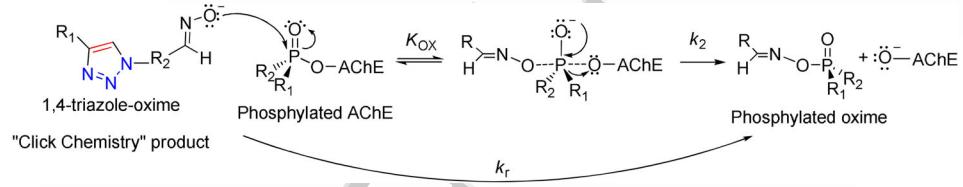

Figure 3. General Scheme of oxime-assisted reactivation of phosphylated AChE and kinetics of reactivation by selected oximes. Mean values from at least three experiments are presented. Reactivation constants were determined by nonlinear regression of experimental data and are presented in Table 1.

(low dissociation constant) of oxime for the phosphorylated enzyme. On the other hand, the highest reactivation rate (k_2) that was evaluated for oxime **1B**, was coupled with a low binding affinity ($1/K_{OX}$) for the phosphoramidate conjugated AChE, resulting in a compromised overall reactivation rate (k_r). Nevertheless, five of the most efficient reactivators of tabun-phosphorylated AChE are triazole oximes with an aldoxime-positioned *ortho*- to the quaternary pyridinium nitrogen or at the 2-position of the imidazolium ring. Out of 8 bis-quaternary reactivators, 6 oximes have two quaternary nitrogen atoms in an extended distance of 8.4 Å, equivalent to 8 methylenes, two oximes have distances corresponding to 7 methylenes and one has a distance corresponding to 6 methylenes. A distance of ≈8 Å or more between the two quaternary nitrogens enables optimal positioning of the oxime molecule in the phosphoramidated AChE gorge. Moreover, the highest k_r was achieved by oximes **3A** and **9A**, that have two quaternary nitrogens separated by ≈8.4 Å primarily resulting from their low K_{OX} (Table 1)—a value at least 10-fold lower than that of TMB-4 or bis-quaternary pyridinium aldoximes.[2d,4c,6a,b] Oxime **2A** stands out from several selected mono-pyridinium oximes with high reactivation rate and moderate affinity. Its overall reactivation rate is comparable to the most efficient reactivators of tabun-inhibited AChE–bis-pyridinium K048, K074, K075 and K203[4c,6a,c,10] and uncharged reactivators.[11] Although prior computational analyses of bis-pyridinium oximes for optimal tabun reactivation indicate the oxime group should be in the *para*-position on the pyridinium ring,[6b] our results show that it is not the case for this group of oximes, since out of the oximes analyzed herein, only **14A** and **4A** have one oxime group in *para*-position on the pyridinium ring (Table 1).

The absorption spectral analyses and estimation of pK_a values given in Figure 4 show that nucleophilicity of three lead oximes is similar to the pK_a value of the *ortho*-pyridinium oximes such as HI-6.[12] Therefore, for reactivation of tabun-inhibited AChE, an altered orientation and an angle of the oxime group with an *anti*-regioisomer orientation promote more efficient reactivation kinetics.

Screening of oximes as broad-spectrum reactivators of VX-, sarin-, cyclosarin-, and paraoxon-inhibited AChE

While no currently used oxime is sufficiently effective against all nerve agents and pesticides, they show substantially different rate constants depending on the conjugated organophosphate. Since oximes selected from this study exhibited the po-

Table 1. Reactivation kinetic analysis of tabun-inhibited AChE with the most efficient oximes.[a]

Oxime	Oxime Structure	Chemical Name	k_2 [min^{-1}]	K_{OX} [mM]	k_r [$M^{-1}min^{-1}$]	$React_{max}$ [%]
3A	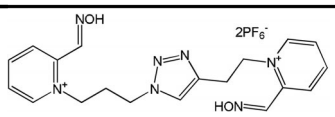	2-((Hydroxyimino)methyl)-1-(3-(4-(2-(2-((hydroxyimino)methyl)pyridinium-1-yl)ethyl)-1*H*-1,2,3-triazol-1-yl)-propyl)pyridinium hexafluorophosphate	0.015 ± 0.001	0.0056 ± 0.0016	3000 ± 630	90
9A	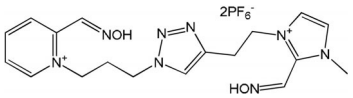	2-((Hydroxyimino)methyl)-1-(3-(4-(2-(2-(hydroxyimino)methyl)-1-methyl-1*H*-imidazol-3-ium-3-yl)ethyl)-1*H*-1,2,3-triazol-1-yl)propyl)pyridinium hexafluorophosphate	0.010 ± 0.001	0.0043 ± 0.0016	2500 ± 1275	80
2A	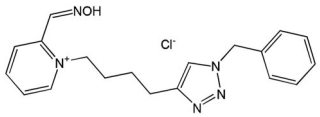	1-(4-(1-Benzyl-1*H*-1,2,3-triazol-4-yl)butyl)-2-((hydroxyimino)methyl)pyridinium hexafluorophosphate	0.026 ± 0.003	0.073 ± 0.036	355 ± 180	100
4A	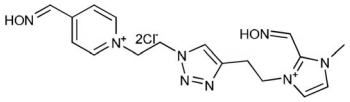	4-((Hydroxyimino)methyl)-1-(2-(4-(2-(2-((hydroxyimino)methyl)-1-methyl-1*H*-imidazol-3-ium-3-yl)ethyl)-1*H*-1,2,3-triazol-1-yl)ethyl)pyridine-1-ium dichloride	0.018 ± 0.001	0.070 ± 0.016	250 ± 57	80
1A	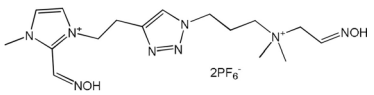	3-(2-(1-(3-((2-(Hydroxyimino)ethyl)dimethylammonio)-propyl)-1*H*-1,2,3-triazol-4-yl)ethyl)-2-((hydroxyimino)-methyl)-1-methyl-1*H*-imidazol-3-ium hexafluorophosphate	0.028 ± 0.002	0.126 ± 0.035	220 ± 65	100
20A	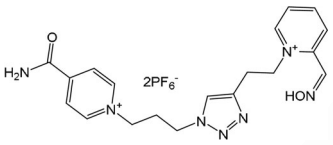	1-(2-(1-(3-(4-Carbamoylpyridinium-1-yl)propyl)-1*H*-1,2,3-triazol-4-yl)ethyl)-2-((hydroxyimino)methyl)pyridinium hexafluorophosphate	0.006 ± 0.0006	0.103 ± 0.041	60 ± 24	60
5A	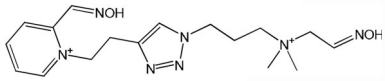	1-(2-(1-(3-((2-(Hydroxyimino)ethyl)dimethylammonio)-propyl)-1*H*-1,2,3-triazol-4-yl)ethyl)-2-((hydroxyimino)-methyl)pyridinium hexafluorophosphate	0.014 ± 0.002	0.29 ± 0.25	47 ± 42	80
14A	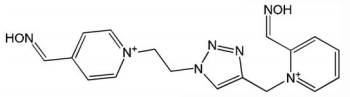	2-((Hydroxyimino)methyl)-1-((1-(2-(4-((hydroxyimino)-methyl)pyridinium-1-yl)ethyl)-1*H*-1,2,3-triazol-4-yl)methyl)pyridinium hexafluorophosphate	0.011 ± 0.002	0.24 ± 0.11	45 ± 21	90
15A	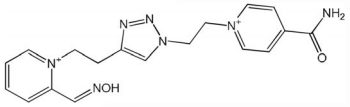	1-(2-(1-(2-(4-Carbamoylpyridinium-1-yl)ethyl)-1*H*-1,2,3-triazol-4-yl)ethyl)-2-((hydroxyimino)methyl)pyridinium hexafluorophosphate	0.013 ± 0.003	0.39 ± 0.33	33 ± 30	70
2B	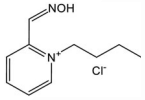	1-Butyl-2-((hydroxyimino)methyl)pyridinium chloride	0.020 ± 0.002	0.82 ± 0.19	25 ± 6.1	90
1B	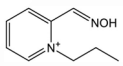	2-((Hydroxyimino)methyl)-1-propylpyridinium chloride (1B)	0.033 ± 0.008	3.9 ± 1.7	8.5 ± 4.3	80

[a] Kinetic parameters (± S.E.): the maximal first-order reactivation rate constant (k_2), the apparent dissociation constant of the conjugated enzyme-oxime reversible complex (K_{OX}), the overall second-order reactivation rate constant (k_r) and maximal percentage of reactivation ($React_{max}$) were determined from at least three experiments.

tential to reactivate tabun-inhibited AChE, a conjugate that is particularly resistant to reactivation, we examined the 19 most potent reactivating oximes for tabun as reactivators of VX-, sarin-, cyclosarin- and paraoxon-inhibited AChE. As presented in Figure 5, several of the selected oximes exhibit reasonable reactivation rates and maximal activities for the tested organophosphates revealing an activity spectrum of universal reactivation. For example, the bis-pyridinium aldoxime **14A** displays a high potency to reactivate both phosphonate and phosphorate AChE conjugates. Moreover, several of these oximes reactivate conjugated AChE more efficiently than the standard reference oxime, 2-PAM, but may lack the wide spectrum of potency of HI-6[11c] on phosphorates and methylphosphonates.

Cytotoxicity

Since the CNS, peripheral autonomic synapses, and the neuromuscular junction are the primary sites of organophosphate inhibition and oxime reactivation, we have chosen a neuroblastoma cell line SH-SY5Y for initial cytotoxicity screens. For testing, we have selected oximes **2A**, **3A**, and **14A** that display different reactivation potencies, as demonstrated by the kinetic constants presented in Table 1 and Figure 3. Oximes were assayed in concentrations up to 800 μM, and the results are presented in Figure 6.

As shown, the maximum percentage inhibition of cell-growth and differentiation was about 20% and occurred only

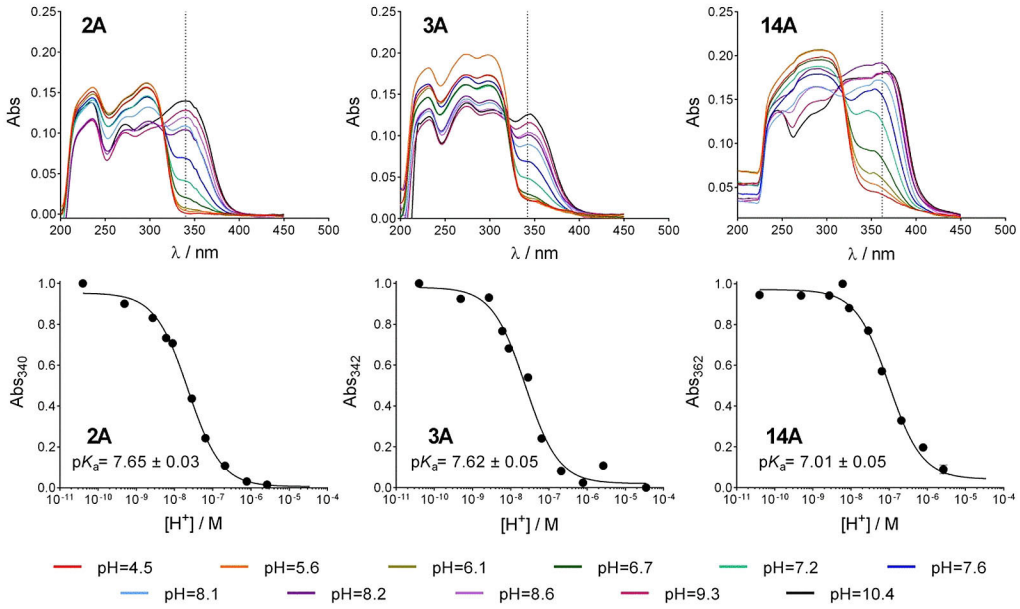

Figure 4. Absorption spectra at 25 °C and pH-dependence of normalized absorbance wherefrom the pK_a values of the oxime group for oximes **2A**, **3A** and **14A** were evaluated (goodness of the fit was $R^2 > 0.99$).

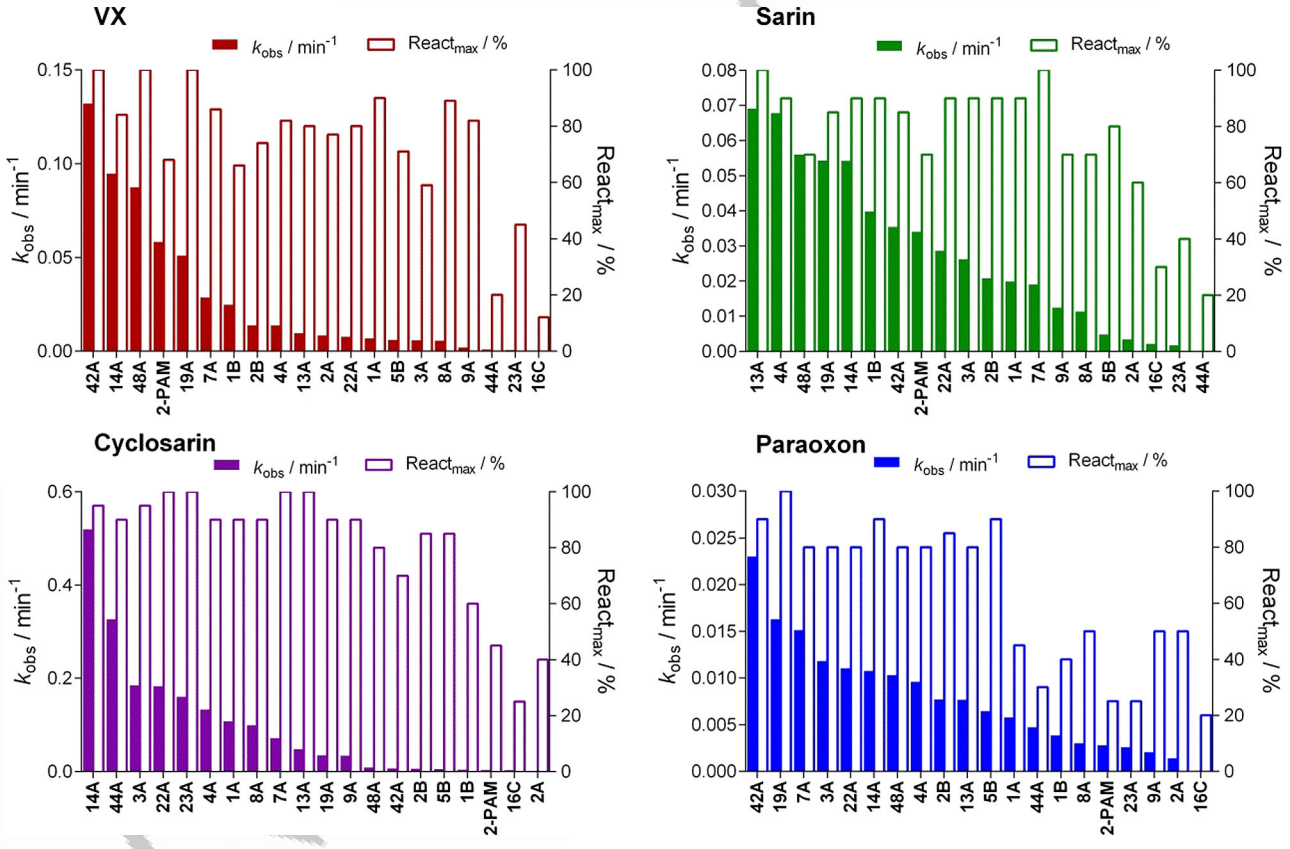

Figure 5. Reactivation screening of AChE inhibited by VX, sarin, cyclosarin and paraoxon by selected 0.1 mM oximes. Observed first order reactivation rates (k_{obs}) are compared to 2-PAM. Presented values are means of at least three experiments (standard errors were less than 10%).

for the highest oxime concentration tested, a concentration level exceeding those employed for in vitro reactivation assays. Practically, a dose-response relationship was not evident in the studied concentration range, so the lead oximes appeared not to show significant cytotoxicity. Therefore, despite these oximes presenting a new structural scaffold, the absence of

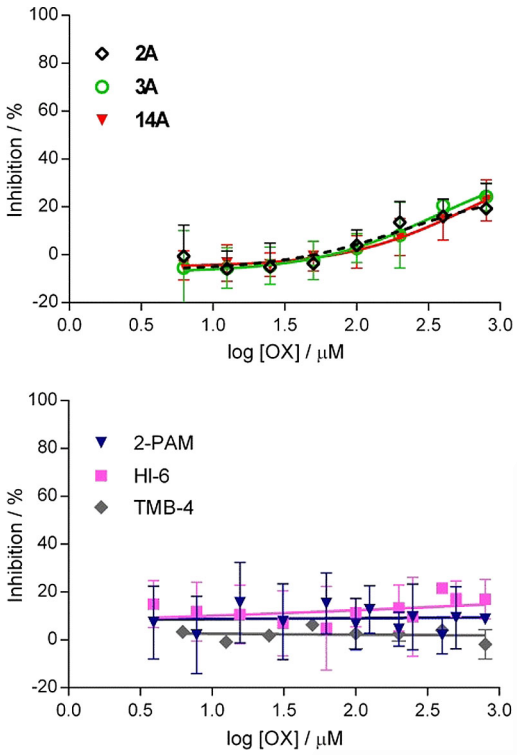

Figure 6. Cytotoxicity of oximes on SH-SY5Y cells plotted as a logarithmic function of concentration. The results were expressed as a percentage of inhibition of cell growth compared with control (non-treated) cells.

toxicity in the neuronal cell assay is comparable to standard oximes as well as to the bis-pyridinium oximes: TMB-4, ICD-585 or K048.[6b]

Pharmacokinetics of lead reactivators of phosphorylated AChE

Oximes **2A**, **3A** and **14A**, with the high reactivation rates and moderate binding affinities, emerged as the lead reactivators of tabun-inhibited AChE, and were chosen for further pharmacokinetic and antidotal testing in mice. Since these oximes are quaternary cations, rapid glomerular filtration and renal tubular secretion are expected, as it was previously shown for similar pyridinium aldoximes.[13] The clearance profile (Figure 7), shows that at 5 mg kg^{-1} injected intramuscularly, most of the initial concentration was eliminated from mice plasma within 60 min. A low volume of distribution, where the antidote is confined to extracellular compartments, seems contributory. In any event, clearance is rapid and multiphasic, but the rapid clearance (short half-life) persists for close to an hour, where the plasma concentration is 10% or less of the original value. This short resident time in the plasma and rapid clearance would require multiple dosing for a sustained therapeutic action of a long-acting organophosphate.[14] It is noteworthy to mention that typically upon intramuscular (i.m.) administration of a quaternary oxime, there is a short redistribution phase followed by the kinetics of elimination from the plasma. That redistribution phase probably takes place within 15 min, a time when the first point was taken. An extrapolation of concentration to zero time yields values of ≈9000 ng mL^{-1} or 9 mg L^{-1} for **3A** and **14A**; this yields a Volume of Distribution of about 0.55 L kg^{-1}, which is reasonable for a quaternary agent. For oxime **2A** the extrapolation value might be closer to 2000 ng mL^{-1} or 2 mg L^{-1}. This finding may implicate sequestration of some of the **2A** compound or a more rapid and complete redistribution phase. Based on these initial findings, a more complete pharmacokinetic analysis, involving plasma and tissue levels with a single lead, phosphoramide-effective oxime seems warranted.

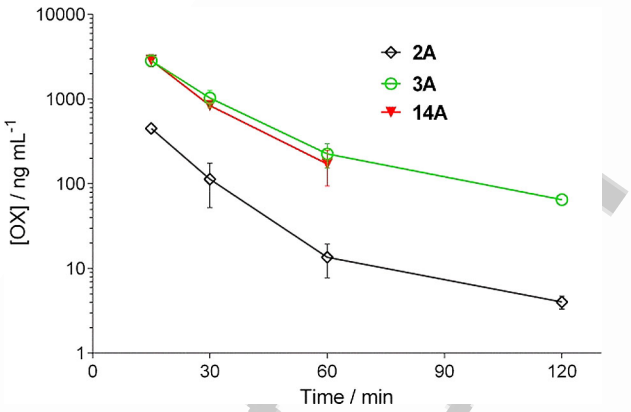

Figure 7. Oxime clearance profile upon i.m. administration of 5 mg kg^{-1} of three oximes in mouse plasma (mean of 3 mice per group and time point). Limits of detection were ≈2 ng mL^{-1}, 50 ng mL^{-1} and 100 ng mL^{-1} for **2A**, **3A** and **14A**, respectively.

Antidotal activity of these oximes in OP-exposed mice

We evaluated in vivo antidotal activity of the oximes in therapy against tabun and four other OPs. The antidotal action of oximes in mice was tested in these early studies by intraperitoneal (i.p.) administration of oxime admixed with atropine one min after subcutaneous (s.c.) OP exposure (Table 2). The

Table 2. Antidotal efficacy of oximes applied at 5 or 25% of their LD_{50} after OP exposure of mice by administering the oxime (i.p.) with atropine (10 mg kg^{-1}) 1 min after OP (s.c.).[a]

Oxime	Oxime LD_{50} [mg kg^{-1}]	Oxime dose [μmol kg^{-1}]	Protective Index (MD) Tabun	VX	Sarin	Paraoxon	Soman
2A	26.7	1.4	2.2 (1.6)	6.4 (5.0)	1.6 (1.3)	11.6 (7.9)	2.5 (1.6)
		7.1	8.9 (4.0)	9.4 (6.3)	2.1 (1.6)	11.2 (7.9)	3.8 (2.5)
3A	8.4	0.63	1.6 (1.0)	5.8 (5.0)	1.4 (1.3)	14.7 (6.3)	1.8 (1.3)
		3.1	8.9 (7.9)	6.8 (6.3)	4.0 (2.0)	11.6 (10.0)	1.8 (1.6)
14A	18.5	3.6	1.5 (1.3)	8.9 (7.9)	2.0 (1.6)	13.6 (10.0)	2.2 (1.6)
		19	5.0 (3.2)	10.3 (10.0)	5.4 (2.0)	14.7 (10.0)	2.5 (2.0)
TMB-4	89.8	13	3.4 (2.5)				
		63	4.0 (2.0)				

[a] LD_{50}—acute toxicity (i.p.) was based upon 24 h mortality rates. Protective Index was the ratio of LD_{50} between OP with antidote and OP given alone. Maximal dose of OP, MD, is the highest multiple of the LD_{50} of OPs, which was fully counteracted by the antidote.

oximes showed significant acute toxicity. However, all three selected oximes (**2A**, **3A** and **14A**) showed better antidotal efficacy than TMB-4 with either dose (5% or 25% of oxime's LD_{50}), giving a satisfactory in vivo Protective Index after exposure to tabun.[6a] When combined with atropine, **3A** ensured survival of all mice against $7.9\times LD_{50}$ of tabun or 2.4 mg kg^{-1}. The administration of a single atropine dose of 10 mg kg^{-1} one minute after tabun resulted in the Protective Index of 1.3. For other nerve agent poisoning, therapy with atropine alone resulted in a Protective Index below 2.[1b] Despite their toxicity, tested oximes provides significant protection against the lethal effects of tabun, presumably due to their enhanced reactivation capacity for tabun-phosphorylated AChE and to concomitant inhibition of unconjugated AChE that may protect residual active AChE from irreversible phosphorylation. It is worthwhile to note that these Protective Indices were obtained by an up to 20-fold lower dose of triazole oximes than for TMB-4, selected on the basis of their acute toxicity and LD_{50} (Table 2). Out of three tested oximes, **14A** provided the greatest antidotal potential in treatment upon exposure to the other OPs and ensured survival of all mice against $10\times LD_{50}$ of VX and paraoxon. The antidotal action of tested compounds appears related to the reactivation kinetics of phosphylated AChE, since their reactivating efficacy shown in vitro (Figure 5) corresponds to their therapeutic efficacy in vivo (Table 2). Further examination of the Protective Indices, administering a lead oxime antidote against the phosphoramidate nerve agents by i.m. administration at various times after OP exposure, should now be considered.

Discussion

Our study has identified a series of oximes with a high propensity for reactivation of human recombinant AChE inhibited by organophosphates. The organophosphate conjugates resemble transition state analogues of acyl ester catalysis, forming relatively stable conjugates of cholinesterases and other serine hydrolases.[15] As found initially by Irwin Wilson and colleagues, nucleophilic oximes, that are site-directed, show a preferential activity as reactivating agents.[16] While most of the alkylphosphate inhibitors of AChE are either phosphorates or methylphosphonates, tabun is unique in representing the phosphoramidates. Hence, the differing chemistry of the phosphoramidates, while forming a tetrahedral conjugate, presents a free electron pair on the phosphoramide nitrogen. Also, the substantial steric hindrance of the dimethylamido group may influence the resistance of tabun to reactivation by certain oximes. Moreover, the phosphoramides have two potential modes of ageing in contrast to the alkyl methylphosphonates and phosphorates.[17]

Recently, a new set of highly toxic phosphoramidates were brought to light through an attempted homicide, with a compound in the Novichok series bearing a fluoride leaving group.[18] The triazole compounds synthesized here and screened in terms of reactivation of the tabun conjugate, in relation to other methylphosphonate and alkyl phosphorate conjugates, suggest that they could serve as lead countermeasures for tabun and other phosphoramidate exposure. The lead reactivators contain an aldoxime substituted *ortho*- to the methylpyridinium nitrogen or a 2-methylimidazole aldoxime moiety. Our study has included reactivation measurements of AChE inhibited by common nerve agents, VX, sarin and cyclosarin, and pesticides forming a toxicant analogous to paraoxon, along with initial assessments of their toxicity in cell culture and mice. Novel reactivators, or recently developed non-oxime reactivators, while showing generally broad activity towards the phosphorates and phosphonates good activity, and potential to penetrate CNS exhibit limitations toward reactivation of the tabun conjugate.[19] As pyridinium and imidazolium aldoximes, they are not likely to cross the blood–brain barrier rapidly, conferring their antidotal activity only to the peripheral nervous system and not the CNS.[6c, 13e, 20] As quaternary ammonium compounds, they are likely to be rapidly cleared by the kidneys, similar to other pyridinium aldoximes. Also, their antidotal activity towards inhaled sarin in a primate system has yet to be examined as has been the case for sarin exposure followed by the antidotal actions of zwitterionic, non-quaternary oximes, such as RS194B.[21]

Conclusions

We have synthesized and pharmacologically characterized a substantial number of 1,2,3-triazole-linked *N*-methylpyridinium and 2-methylimidazolium oximes with significantly improved in vitro reactivating efficacies for tabun-inhibited AChE, when compared to standard bis-pyridinium oximes. This underscores the importance of an efficient cyclization azide-alkyne CuAAC process in forming congeneric libraries of triazole test compounds. Pharmacokinetic properties of the lead compounds were monitored in initial studies in mice, and in vivo antidotal efficacy for three leads was established in tabun-exposed mice. To assess the spectrum of activity, we selected nineteen of the most efficient tabun reactivators to test their efficacy in reactivating AChE inhibited with other OPs. Although several of the tabun antidote leads showed reasonable potency in reactivating other tested AChE-OP conjugates, a universally superior antidote against all organophosphates was not identified. Multidimensional and hydrogen bonding constraints in the AChE active center gorge conjugated with methylphosphonates, phosphorates and phosphoramidates, mitigate against the likelihood of finding a single reactivator most efficient for tabun, sarin, VX, cyclosarin, paraoxon and their congeners. Nevertheless, our findings offer a valuable and comprehensive platform for further development of antidotes and scavengers against tabun and related phosphoramidate exposures, such as the Novichok series of compounds used in poisoning in Salisbury, England in the Spring of 2018.[18]

Experimental Section

■■The lengthy characterization details have been removed from the main manuscript as they were a direct repeat of the Supporting Information. A line has been added to direct readers to this for further information■■

Chemistry. The majority of oximes were synthesized by Cu^{I}-catalyzed azide-alkyne cycloaddition to form the *anti*-triazole using a library of small molecule building blocks, as shown in Figure 1. 1H and 13C NMR spectra were recorded on a Varian INOVA-400 spectrometer in CDCl3 (7.26 ppm for 1 H, 77.00 ppm 13C), [D_6]DMSO (2.50 ppm for 1 H, 39.43 ppm for 13C) as standards. Reagents and solvents were purchased from Aldrich, Acros or GFS and used without further purification. Full details on experimental procedures and characterization are available in the Supporting Information.

Chemicals. Tabun, VX, sarin, cyclosarin, and soman were purchased from NC Laboratory, Spiez, Switzerland. Nerve agent stock solutions were prepared in isopropyl alcohol, while further dilutions were made in water immediately prior to use. Paraoxon ethyl (Sigma–Aldrich, St. Louis, MO, USA) was diluted in ethanol just before use. Acetylthiocholine iodide (ATCh), standard oximes and 5,5′-dithio-bis(2-nitrobenzoic acid) (DTNB) were purchased from Sigma Chemical Co., St. Louis, MO, USA. Stock solutions of oximes were prepared in water or dimethyl sulfoxide (DMSO; Kemika, Zagreb, Croatia) and diluted in sodium phosphate buffer (0.1 M, pH 7.4) just before use. Atropine sulfate was purchased from Kemika, Zagreb, Croatia.

Cholinesterase activity measurements. Recombinant human AChE (AChE), wild type, was prepared as described earlier.[7c] For reactivation experiments, the enzyme was incubated with a ten-fold excess of OP until inhibition was greater than 95%. Such inhibited enzyme was passed through a Sephadex G-50 spin column (Roche Diagnostic GmbH, Mannheim, Germany) to remove an excess of unconjugated OP. After gel filtration by centrifugation, enzyme was diluted 10-fold in 0.1 M sodium phosphate buffer, pH 7.4, containing 0.01% BSA and incubated with oxime at 25 °C. At specified time intervals, an aliquot was diluted 100-fold in phosphate buffer containing DTNB; upon addition of ATCh, residual enzyme activity was measured. Final concentrations of ATCh and DTNB in the assay were 1.0 and 0.3 mM, respectively. An equivalent sample of uninhibited enzyme was passed through a parallel column, diluted to the same extent as the inhibition mixture, and control activity was measured in the presence of oxime at concentrations used for reactivation. Both activities of control and reactivation mixture were corrected for oxime-induced hydrolysis of ATCh. Reactivation of the enzyme was measured immediately upon addition of ATCh at nine time points until reaching maximal percentage of reactivation ($React_{max}$). Reactivation screening was conducted at a given oxime concentration (0.1 or 1 mM) up to 24 h, wherefrom the observed first-order reactivation rate constant (k_{obs}) and maximal percentage of reactivation ($React_{max}$) were determined as previously described.[23] More detailed reactivation kinetics using a wider oxime concentration range enables the determination of reactivation constants: k_2 (maximal first-order reactivation rate constant), K_{ox} (apparent phosphylated enzyme-oxime dissociation constant) and k_r (second-order reactivation rate constant) as described previously.[9b]

All cholinesterase activity measurements were performed in 0.1 M sodium phosphate buffer containing 0.01% BSA, pH 7.4 at 25 °C using the Ellman spectrophotometric method[24] at 412 nm on a CARY 300 spectrophotometer (Varian Inc., Australia) with temperature controller.

pK_a determination of selected oximes. Protonation of ionizable groups in the oximes was monitored by UV-VIS spectrometry (CARY 300 spectrophotometer, Varian Inc., Australia) and proton dissociation constants were determined from pH-absorbance profiles at 25 °C using Equation (1) as described earlier.[12]

$$A_{tot} = \frac{A_1 \cdot [H^+] + A_2 \cdot K_a}{[H^+] + K_a} \quad (1)$$

The observed absorbance at maximum absorption wavelength A_{tot} is the sum of the absorption fractions of all aldoxime ionization states present. A_1 and A_2 are absorbances of the species with protonated (HL^+) and deprotonated (L) oxime group, respectively.

Cytotoxicity assay. SH-SY5Y cells were obtained from ATCC LGC Standards GmbH, Germany, and cultured according to the protocol in DMEM F12 medium (2 mM glutamine + 1% non-essential amino acids + 15% fetal bovine serum, Sigma–Aldrich, Germany). Two days before the toxicity study, cells were seeded on 96 F-bottom clear well plates in 1×10^5/ well. On the day of the experiment, medium was removed and fresh medium containing oximes in a designated concentration was added (120 μL volume per well). Oximes were tested at eight concentrations; in a 1:2 dilution sequence, starting from 800 μM. Plates were incubated for 24 h at 37 °C. After incubation, cells were washed twice with PBS and the MTS reagent was added to determine cytotoxic activity according to the manufacturer's protocol (CellTiter 96 AQueous One Solution Cell Proliferation Assay, Promega, USA). The MTS detection reagent assays succinate dehydrogenase mitochondrial activity of living cells.[25] Absorbances were read at 490 nm on a plate reader spectrophotometer (InfiniteM200 Pro, Tecan, USA), and results were expressed as the percentage of inhibition compared to control cells. Total percentage of DMSO in cytotoxicity assay was 0.8% and did not appear to influence the test. Data were evaluated using predefined IC_{50} equation from a GraphPad Prism program (San Diego, USA).

Oxime pharmacokinetics in mice. Female CD-1 mice, 4–8 weeks old (22–34 g body weight), were purchased from Harlan (Livermore, CA). Mice were fed Purina Certified Rodent Chow #5002 food and purified water was provided *ad libitum*. Mice were kept in hanging polycarbonate cages at 21–23 °C, exchanging light and dark cycles every 12 h. General procedures for animal care and housing were in accordance with the National Research Council (NRC) Guide for the Care and Use of Laboratory Animals (1996) and the Animal Welfare Standards incorporated in 9 CFR Part 3, 1991. For pharmacokinetic experiments mice were divided into groups of three, and 5 mg kg^{-1} of the oximes was administered i.m. in a single dose. Three animals were injected for each time point analyzed. Blood (≈300 μL) was collected from the retro-orbital sinus of mice under isoflurane anesthesia into tubes containing EDTA, processed to plasma within 30 minutes of collection, and then stored frozen at ≤ −80 °C (± 10 °C). Concentrations of the oxime in body compartments were determined by LC-MS using multiple reaction monitoring (MRM) electrospray ionization detection in positive ion mode as described previously.[26]

Antidotal tests in OP exposed mice. Male NIH/OlaHsd mice (20–25 g body weight; purchased from Imunološki zavod, Zagreb, Croatia) were fed a standard diet, had free access to water and were kept in Macrolone cages at 21 °C, exchanging light and dark cycles every 12 h. For the experiments mice were divided into groups of four. Acute toxicity (LD_{50}) was based upon 24 h mortality rates and 95% confidence limits were estimated from data tables, as described elsewhere.[27] Antidotal activity of oximes in OP-exposed mice was tested by administration (i.p.) of selected oxime (in doses of 5% or 25% of its LD_{50}) dissolved in the solution of atropine sulphate (10.0 mg kg^{-1} b.w.), one minute after OP exposure (s.c.). Antidotal efficacy was expressed as a Protective Index (PI) with 95% confidence limits and maximal dose of OP (MD). The PI is the ratio of LD_{50} between OP with treatment and OP given alone, without treatment. The MD is the highest multiple of the OP's LD_{50}, that

was fully counteracted by treatments. The mice described in these experiments were treated in accord with the approval of the Ethics Committee of the Institute for Medical Research and Occupational Health in Zagreb, Croatia.

Appendix

For reactivation screening results of the tabun-inhibited AChE, see Table 3.

Table 3. Reactivation screening of the tabun-inhibited AChE by A) sixty-two triazole compounds, B) five *N*-alkyl-2 pyridinium compounds, C) seventeen compounds with more complex *N*-alkyl substitutions, D) twenty-seven miscellaneous oximes, 2-PAM, and obidoxime. The reactivation rate at the given oxime concentration, k_{obs} (1 mM; except for 12 oximes as marked in the table), maximal percentage of reactivation, $React_{max}$ obtained in time (*t*), and reversible inhibition by the oxime (in concentration 100-fold lower than employed in reactivation) were evaluated. Reactivation was monitored up to 24 h.

A) Triazole compounds		k_{obs} [min^{-1}]	$React_{max}$ [%]	*t* [h]	**Inhibition [OX]**
1A	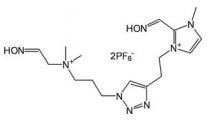	0.0270	95	1.5	40% (0.01 mM)
2A	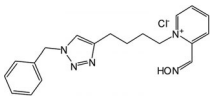	0.0260	95	2.5	65% (0.01 mM)
3A (0.2 mM)	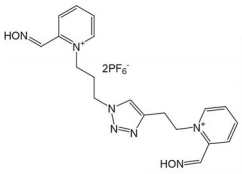	0.0170	80	3	55% (0.002 mM)
4A	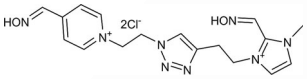	0.0160	85	4	60% (0.01 mM)
5A	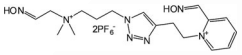	0.0153	95	4	20% (0.01 mM)
6A	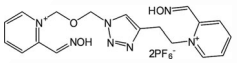	0.0150	90	4	85% (0.01 mM)
Obidoxime[8]	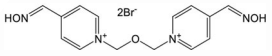	*0.0150*	*85*	*4*	*11% (0.01 mM)*
7A	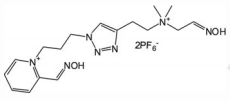	0.0140	80	6	40% (0.01 mM)
8A	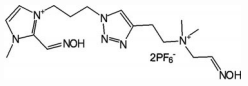	0.0136	85	5	70% (0.01 mM)
9A (0.1 mM)	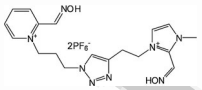	0.0099	75	4	55% (0.001 mM)
10A	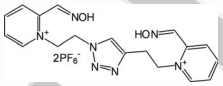	0.0093	100	7	40% (0.01 mM)
11A	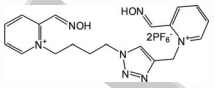	0.0091	95	7	85% (0.01 mM)
12A	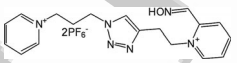	0.0090	95	7.5	63% (0.01 mM)
13A	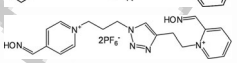	0.0088	80	6	70% (0.01 mM)
14A	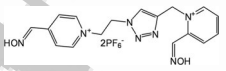	0.0085	90	6	45% (0.01 mM)
15A	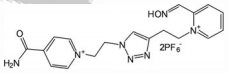	0.0085	60	4	20% (0.01 mM)
16A	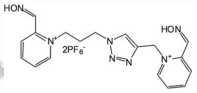	0.0083	90	7	75% (0.01 mM)

Table 3. (Continued)

17A	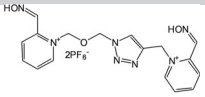	0.0083	90	7	80% (0.01 mM)
18A	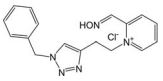	0.0078	90	7	80% (0.01 mM)
19A	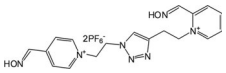	0.0068	80	8	30% (0.01 mM)
20A	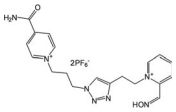	0.0061	45	4	70% (0.01 mM)
21A	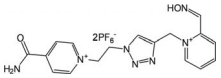	0.0050	65	7	30% (0.01 mM)
22A (0.1 mM)	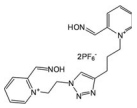	0.0050	50	8	30% (0.001 mM)
23A (0.1 mM)	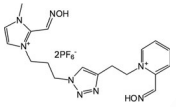	0.0043	80	10	70% (0.001 mM)
24A	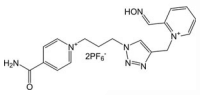	0.0036	65	12	70% (0.01 mM)
25A (0.1 mM)	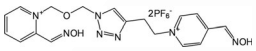	0.0035	80	11	75% (0.001 mM)
26A	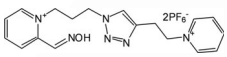	0.0029	55	12	80% (0.01 mM)
27A	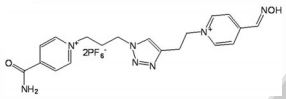	0.0027	55	12	30% (0.01 mM)
28A	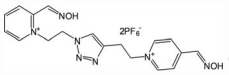	0.0027	50	12	40% (0.01 mM)
2-PAM		*0.0026*	*80*	*24*	*10% (0.01 mM)*
29A	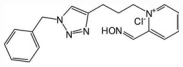	0.0024	80	24	60% (0.01 mM)
30A	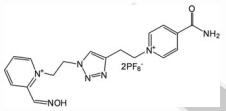	0.0023	50	24	30% 0.01 mM)
31A	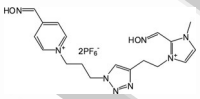	0.0022	90	24	85% (0.01 mM)
32A	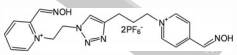	0.0022	75	24	80% (0.01 mM)
33A	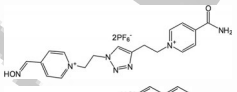	0.0022	60	24	15% (0.01 mM)
34A	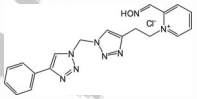	0.0019	90	24	30% (0.01 mM)
35A	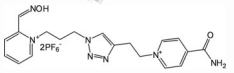	0.0018	40	24	85% (0.01 mM)
36A	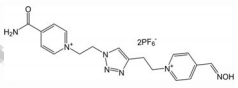	0.0017	55	24	25% (0.01 mM)

Table 3. (Continued)

37A	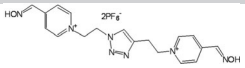	0.0017	35	24	40% (0.01 mM)
38A (0.8 μM)	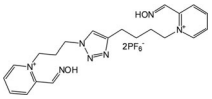	0.0016	45	24	10% (8 nM)
39A	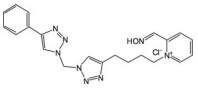	0.0014	80	24	30% (0.01 mM)
40A (0.1 mM)	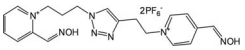	0.0013	40	24	85% (0.001 mM)
41A	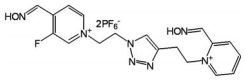	0.0013	40	24	20% (0.01 mM)
42A	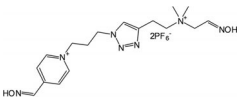	0.0012	50	24	55% (0.01 mM)
43A	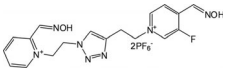	0.0011	35	24	30% (0.01 mM)
44A (20 μM)	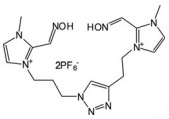	0.0010	40	24	45% (0.2 μM)
45A	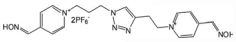	0.0009	65	24	60% (0.01 mM)
46A	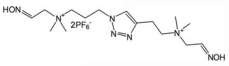	0.0009	55	24	15% (0.01 mM)
47A	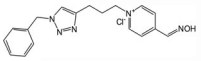	0.0008	55	24	40% (0.01 mM)
48A	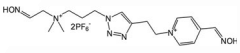	0.0008	50	24	40% (0.01 mM)
49A	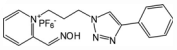	0.0008	45	24	20% (0.01 mM)
50A	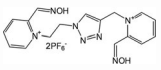	0.0006	50	24	60% (0.01 mM)
51A (0.8 μM)	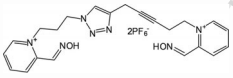	–	≤20	24	10% (8 nM)
52A	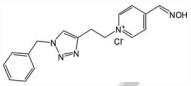	–	≤20	24	20% (0.01 mM)
53A	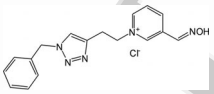	–	≤20	24	30% (0.01 mM)
54A (0.1 mM)	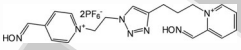	–	≤20	24	40% (0.001 mM)
55A	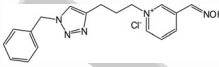	–	≤20	24	40% (0.01 mM)
56A (0.8 μM)	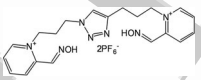	–	≤20	24	40% (8 nM)
57A	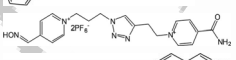	–	≤20	24	45% (0.01 mM)
58A	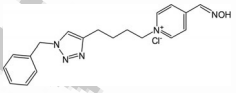	–	≤20	24	45% (0.01 mM)
59A	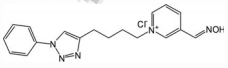	–	≤20	24	70% (0.01 mM)
60A	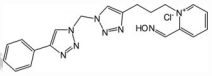	–	≤20	24	80% (0.01 mM)

Table 3. (Continued)

61A	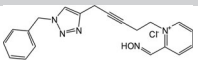	–	≤20	24	80% (0.01 mM)
62A (0.1 mM)	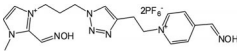	–	≤20	24	85% (0.001 mM)
B) *N*-alkyl-2-pyridinium compounds		k_{obs} [min^{-1}]	React$_{max}$ [%]	*t* [h]	Inhibition [OX]
1B	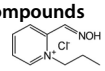	0.0123	90	6	15% (0.01 mM)
2B	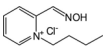	0.0111	85	4	40% (0.01 mM)
3B		0.0089	100	8	5% (0.01 mM)
4B	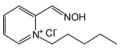	0.0045	65	8	45% (0.01 mM)
5B	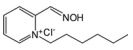	0.0030	70	12	20% (0.01 mM)
2-PAM		*0.0026*	*80*	*24*	*10% (0.01 mM)*
C) Compounds with more complex *N*-alkyl substitutions		k_{obs} [min^{-1}]	React$_{max}$ [%]	*t* [h]	Inhibition [OX]
1C	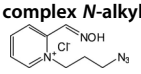	0.0145	95	6	20% (0.01 mM)
2C	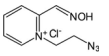	0.0129	85	5	40% (0.01 mM)
3C	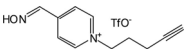	0.0058	90	10	25% (0.01 mM)
4C	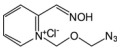	0.0052	80	11	30% (0.01 mM)
5C	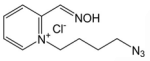	0.0035	75	12	20% (0.01 mM)
6C	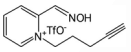	0.0031	70	12	65% (0.01 mM)
2-PAM		*0.0026*	*80*	*24*	*10% (0.01 mM)*
7C	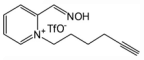	0.0020	70	24	55% (0.01 mM)
8C	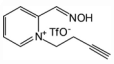	0.0020	60	24	20% (0.01 mM)
9C	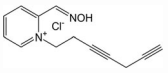	0.0014	50	24	15% (0.01 mM)
10C	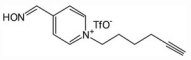	0.0009	55	24	50% (0.01 mM)
11C	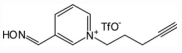	0.0006	50	24	40% (0.01 mM)
12C	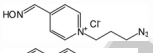	–	≤20	24	5% (0.01 mM)
13C	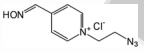	–	≤20	24	5% (0.01 mM)
14C	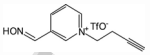	–	≤20	24	10% (0.01 mM)
15C	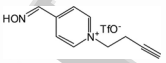	–	≤20	24	10% (0.01 mM)
16C	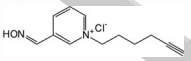	–	≤20	24	60% (0.01 mM)
17C		–	≤20	24	85% (0.01 mM)
D) Miscellaneous oximes		k_{obs} [min^{-1}]	React$_{max}$ [%]	*t* [h]	Inhibition [OX]
1D	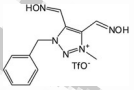	0.0092	100	7	60% (0.01 mM)
2-PAM		*0.0026*	*80*	*24*	*10% (0.01 mM)*
2D	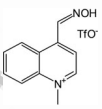	0.0014	90	24	40% (0.01 mM)

Table 3. (Continued)

3D	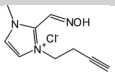	0.0009	60	24	50% (0.01 mM)
4D	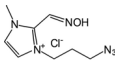	0.0007	40	24	60% (0.01 mM)
5D	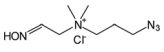	–	≤20	24	5% (0.01 mM)
6D	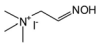	–	≤20	24	10% (0.01 mM)
7D	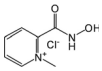	–	≤20	24	10% (0.01 mM)
8D	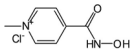	–	≤20	24	10% (0.01 mM)
9D	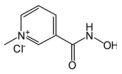	–	≤20	24	10% (0.01 mM)
10D	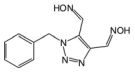	–	≤20	24	10% (0.01 mM)
11D		–	≤20	24	10% (0.01 mM)
12D	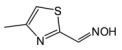	–	≤20	24	10% (0.01 mM)
13D	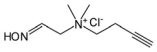	–	≤20	24	15% (0.01 mM)
14D	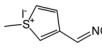	–	≤20	24	20% (0.01 mM)
15D		–	≤20	25	20% (0.01 mM)
16D		–	≤20	24	20% (0.01 mM)
17D	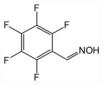	–	≤20	24	20% (0.01 mM)
18D	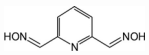	–	≤20	24	20% (0.01 mM)
19D		–	≤20	24	20% (0.01 mM)
20D		–	≤20	24	20% (0.01 mM)
21D		–	≤20	24	20% (0.01 mM)
22D	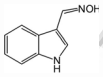	–	≤20	24	30% (0.01 mM)
23D		–	≤20	24	35% (0.01 mM)
24D	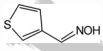	–	≤20	24	35% (0.01 mM)
25D	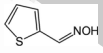	–	≤20	24	40% (0.01 mM)
26D	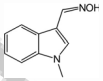	–	≤20	24	40% (0.01 mM)
27D	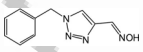	–	≤20	24	40% (0.01 mM)

Acknowledgements

This work was supported by the CounterACT Program, the National Institute of Neurological Disorders and Stroke (NINDS), National Institute of Health (NIH, Grant Number U01 NS058046) and by the Croatian Science Foundation (HrZZ-IP-2013-11-4307).

Conflict of interest

The authors declare no conflict of interest.

Keywords: acetylcholinesterase · biochemistry · heterocycles · nerve agents · organophosphate antidotes

[1] a) P. Taylor in *The Pharmacological Basis of Therapeutics, 13th ed.* (Ed.: L. L. Brunton), McGraw-Hill, New York, **2018**, pp. 163 – 175; b) R. M. Dawson, *J. Appl. Toxicol.* **1994**, *14*, 317 – 331.

[2] a) A. P. L. De Jong, Z. G. Wolring, *Biochem. Pharmacol.* **1984**, *33*, 1119 – 1125; b) F. Worek, R. Widmann, O. Knopff, L. Szinicz, *Arch. Toxicol.* **1998**, *72*, 237 – 243; c) F. Worek, H. Thiermann, L. Szinicz, P. Eyer, *Biochem. Pharmacol.* **2004**, *68*, 2237 – 2248; d) Z. Kovarik, M. Čalić, G. Šinko, A. Bosak, *Arh. Hig. Rada Toksikol.* **2007**, *58*, 201 – 209.

[3] M. Eto in *The Organophosphorus Pesticides* (Ed.: G. Zweig), CRC, Cleveland, **1976**, p. 142.

[4] a) F. Ekström, C. Akfur, A. K. Tunemalm, S. Lundberg, *Biochemistry* **2006**, *45*, 74 – 81; b) F. Ekström, Y. P. Pang, M. Boman, E. Artursson, C. Akfur, S. Börjegren, *Biochem. Pharmacol.* **2006**, *72*, 597 – 607; c) M. Čalić, A. Bosak, K. Kuča, Z. Kovarik, *Chem.-Biol. Interact.* **2008**, *175*, 305 – 308; d) E. Artursson, C. Akfur, A. Hörnberg, F. Worek, F. Ekström, *Toxicology* **2009**, *265*, 108 – 114.

[5] a) M. P. Stojiljković, M. Jokanović, *Arh. Hig. Rada Toksikol.* **2006**, *57*, 435 – 443; b) S. Berend, M. Katalinić, A. L. Vrdoljak, Z. Kovarik, K. Kuča, B. Radić, *J. Enzyme Inhib. Med. Chem.* **2010**, *25*, 531 – 536.

[6] a) M. Čalić, A. L. Vrdoljak, B. Radić, D. Jelić, D. Jun, K. Kuča, Z. Kovarik, *Toxicology* **2006**, *219*, 85 – 96; b) Z. Kovarik, M. Čalić, A. Bosak, G. Šinko, D. Jelić, *Croat. Chem. Acta* **2008**, *81*, 47 – 57; c) Z. Kovarik, A. L. Vrdoljak, S. Berend, M. Katalinić, K. Kuča, K. Musilek, B. Radić, *Arh. Hig. Rada Toksikol.* **2009**, *60*, 19 – 26.

[7] a) H. C. Kolb, K. B. Sharpless, *Angew. Chem. Int. Ed.* **2001**, *40*, 2004 – 2021; *Angew. Chem.* **2001**, *113*, 2056 – 2075; b) H. C. Kolb, K. B. Sharpless, *Drug Discovery Today* **2003**, *8*, 1128 – 1137; c) R. Cochran, J. Kalisiak, T. Kucukkilinc, Z. Radic, E. Garcia, L. Zhang, K. Y. Ho, G. Amitai, Z. Kovarik, V. V. Fokin, K. B. Sharpless, P. Taylor, *J. Biol. Chem.* **2011**, *286*, 29718 – 29724; d) P. Sapkale, M. Sahu, M. Chaudhari, P. R. Patil, *Int. J. Pharm. Pharm. Sci.* **2014**, *6*, 99 – 103.■■Ref. 7d not found with current information, please check. DOI?■■

[8] Z. Kovarik, M. Katalinić, G. Šinko, J. Binder, O. Holas, Y.-S. Jung, L. Musilova, D. Jun, K. Kuča, *Chem.-Biol. Interact.* **2010**, *187*, 167 – 171.

[9] a) L. Wong, Z. Radić, R. J. M. Brüggemann, N. Hosea, H. A. Berman, P. Taylor, *Biochemistry* **2000**, *39*, 5750 – 5757; b) Z. Kovarik, Z. Radić, H. A. Berman, V. Simeon-Rudolf, E. Reiner, P. Taylor, *Biochemistry* **2004**, *43*, 3222 – 3229.

[10] F. Worek, J. von der Wellen, K. Musilek, K. Kuca, H. Thiermann, *Arch. Toxicol.* **2012**, *86*, 1379 – 1386.

[11] a) G. Mercey, T. Verdelet, G. Saint-André, E. Gillon, A. Wagner, R. Baati, L. Jean, F. Nachon, P.-Y. Renard, *Chem. Commun.* **2011**, *47*, 5295 – 5297; b) J. Renou, J. Dias, G. Mercey, T. Verdelet, C. Rousseau, A.-J. Gastellier, M. Arboléas, M. Touvrey-Loiodice, R. Baati, L. Jean, F. Nachon, P.-Y. Renard, *RSC Adv.* **2016**, *6*, 17929 – 17940; c) T. Zorbaz, A. Braïki, N. Maraković, J. Renou, E. de la Mora, N. M. Hrvat, M. Katalinić, I. Silman, J. L. Sussman, G. Mercey, C. Gomez, R. Mougeot, B. Perez, R. Baati, F. Nachon, M. Weik, L. Jean, Z. Kovarik, P.-Y. Renard, *Chem. Eur. J.* **2018**, *24*, 9675 – 9691.

[12] G. Šinko, M. Čalić, Z. Kovarik, *FEBS Lett.* **2006**, *580*, 3167 – 3172.

[13] a) F. R. Sidell, W. A. Goff, *J. Pharm. Sci.* **1971**, *60*, 1224 – 1228; b) R. Kušić, B. Bošković, V. Vojvodić, D. Jovanović, *Fundam. Appl. Toxicol.* **1985**, *5*, 89 – 97■■Ref. 13b not found with current information, please check. DOI?■■; c) J. Z. Karasova, J. Chladek, M. Hroch, F. Josef, D. Hnidkova, K. Kuca, *J. Appl. Toxicol.* **2011**, *33*, 18 – 23; d) S. P. Hong, S. T. Gibb, M. R. Kobs, J. D. Osheroff, B. L. Burban, *Int. J. Toxicol.* **2013**, *32*, 30S – 37S; e) M. Katalinić, N. M. Hrvat, J. Z. Karasová, J. Misik, Z. Kovarik, *Arh. Hig. Rada Toksikol.* **2015**, *6*, 291 – 298.

[14] D. Steinritz, F. Eyer, F. Worek, H. Thiermann, H. John, *Toxicol. Lett.* **2016**, *244*, 121 – 123.

[15] P. Taylor, Z. Radić, *Annu. Rev. Pharmacol. Toxicol.* **1994**, *34*, 281 – 320.

[16] a) I. B. Wilson, S. Ginsburg, *Biochim. Biophys. Acta* **1955**, *18*, 168 – 170; b) H. C. Froede, I. B. Wilson in *The Enzymes, 3rd ed.* (Ed: P. D. Boyer), Academic Press, New York, London, **1971**, pp. 87 – 114.

[17] a) A. Shafferman, A. Ordentlich, D. Barak, D. Stem, N. Ariel, B. Velan, *Biochem. J.* **2008**, *318*, 833 – 844; b) E. Carletti, H. Li, F. Ekstrom, Y. Nicolet, M. Loiodice, E. Gallon, M. T. Froment, O. Lockridge, L. M. Schopfer, P. Masson, F. Nachon, *J. Am. Chem. Soc.* **2008**, *130*, 16011 – 16020; c) O. Tenberken, H. Thiermann, F. Worek, G. Reiter, *Toxicol. Lett.* **2010**, *195*, 142 – 146.

[18] R. Stone, *Science* **2018**, *359*, 1314 – 1315.

[19] a) C. L. Cadieux, H. Wang, Y. Zhang, J. A. Koenig, T.-M. Shih, J. McDonough, J. Koh, D. Cerasoli, *Chem.-Biol. Interact.* **2016**, *259*, 133 – 141; b) R. Sit, Z. Kovarik, N. M. Hrvat, S. Žunec, C. Green, V. V. Fokin, K. B. Sharpless, Z. Radić, P. Taylor, *J. Pharmacol. Exp. Ther.* **2018**, *367*, 363 – 372; c) M. C. de Koning, G. Horn, F. Worek, M. van Grol, *Eur. J. Med. Chem.* **2018**, *157*, 151 – 160; d) T. Zorbaz, D. Malinak, N. Maraković, N. M. Hrvat, A. Zandona, M. Novotny, A. Skarka, R. Andrys, M. Benkova, O. Soukup, M. Katalinić, K. Kuca, Z. Kovarik, K. Musilek, *J. Med. Chem.* **2018**, DOI: https://doi.org/10.1021/acs.jmedchem.8b01398.

[20] M. Katalinić, G. Šinko, N. M. Hrvat, T. Zorbaz, A. Bosak, Z. Kovarik, *Toxicology* **2018**, *406 – 407*, 104 – 113.

[21] a) Y. J. Rosenberg, L. Mao, X. Jiang, J. Lees, L. Zhang, Z. Radic, P. Taylor, *Chem.-Biol. Interact.* **2017**, *274*, 50 – 57; b) Y. J. Rosenberg, L. Mao, X. Jiang, J. Lees, L. Urban, J. D. Momper, Y. Sepulvida, Y. J. Shyong, P. Taylor, *Toxicol. Lett.* **2018**, *274*, 50 – 57.■■Ref. 21b not found with current information, pleas check. DOI?■■

[22] E. Vedejs, D. A. Engler, M. J. Mullins, *J. Org. Chem.* **1977**, *42*, 3109 – 3113.

[23] M. Katalinić, N. M. Hrvat, K. Baumann, S. M. Piperčić, S. Makarić, S. Tomić, O. Jović, T. Hrenar, A. Miličević, D. Jelić, S. Žunec, I. Primožič, Z. Kovarik, *Toxicol. Appl. Pharmacol.* **2016**, *310*, 195 – 204.

[24] G. L. Ellman, K. D. Courtney, V. Andres, Jr., R. M. Featherstone, *Biochem. Pharmacol.* **1961**, *7*, 88 – 95.

[25] T. Mosmann, *J. Immunol. Methods* **1983**, *65*, 55 – 63.

[26] a) Z. Radić, T. Dale, Z. Kovarik, S. Berend, E. Garcia, L. Zhang, G. Amitai, C. Green, B. Radić, B. M. Duggan, D. Ajami, J. Rebek, P. Taylor, *Biochem. J.* **2013**, *450*, 231 – 242; b) Z. Radić, R. K. Sit, Z. Kovarik, S. Berend, E. Garcia, L. Zhang, G. Amitai, C. Green, B. Radić, V. V. Fokin, K. B. Sharpless, P. Taylor, *J. Biol. Chem.* **2012**, *287*, 11798 – 11809.

[27] a) W. R. Thompson, *Bacteriol. Rev.* **1947**, *11*, 115 – 145; b) C. S. Weil, *Biometrics* **1952**, *8*, 249 – 263.

Manuscript received: October 7, 2018
Revised manuscript received: November 9, 2018
Accepted manuscript online: November 20, 2018
Version of record online: ■■ ■■, 0000

FULL PAPER

Developing antidotes: A substantial number of *N*-methylpyridinium and 2-methylimidazolium oximes that show significantly improved in vitro reactivating efficacies for tabun-inhibited AChE have been synthesized and pharmacologically characterized. These findings offer a valuable and comprehensive platform for further development of antidotes and scavengers against tabun and related phosphoramidate exposures.

Nerve Agents

*Z. Kovarik, J. Kalisiak, N. M. Hrvat, M. Katalinić, T. Zorbaz, S. Žunec, C. Green, Z. Radić, V. V. Fokin, K. B. Sharpless, P. Taylor**

■■ – ■■

Reversal of Tabun Toxicity Enabled by a Triazole-Annulated Oxime Library—Reactivators of Acetylcholinesterase

Please check that the ORCID identifiers listed below are correct. We encourage all authors to provide an ORCID identifier for each coauthor. ORCID is a registry that provides researchers with a unique digital identifier. Some funding agencies recommend or even require the inclusion of ORCID IDs in all published articles, and authors should consult their funding agency guidelines for details. Registration is easy and free; for further information, see http://orcid.org/.

Dr. Zrinka Kovarik
Dr. Jarosław Kalisiak
Dr. Nikolina Maček Hrvat
Dr. Maja Katalinić
Tamara Zorbaz
Dr. Suzana Žunec
Dr. Carol Green
Dr. Zoran Radić
Dr. Valery V. Fokin
Prof. K. Barry Sharpless
Prof. Palmer Taylor http://orcid.org/0000-0002-3081-131X